

# A Dimensionality Reduction MUSIC Method for Joint DOA and Polarization Estimation in the PRDRF System Using SSSC-EVSA

Pinjiao Zhao<sup>1, \*</sup>, Guobing Hu<sup>1</sup>, and Liwei Wang<sup>2</sup>

**Abstract**—Traditional long vector-based MUSIC methods require 4D spectral search, which suffers from heavy computational complexity. This paper develops a joint DOA and polarization estimation method named as dimensionality reduction MUSIC (DR-MUSIC) method for a passive radar direction finding (PRDRF) system using spatially separated single-component circular electromagnetic vector sensor array (SSSC-EVSA), where 4D spectral search is transformed into 2D spectral search by exploiting rank deficiency of the signal component of cost function. Polarization parameters are estimated via the generalized eigenvector of matrix pencil, which can be utilized for the recognition of radar and decoy. In addition, the estimation performance of the proposed DR-MUSIC method is also studied considering the phase inconsistency among multi-channels. Simulation results demonstrate the effectiveness of the DR-MUSIC method.

## 1. INTRODUCTION

Direction of arrival (DOA) estimation [1–3] has been a key issue in a passive radar direction finding (PRDRF) system. Electromagnetic vector sensor array (EVSA), which can take advantage of the polarization diversity of the impinging sources, has shown significant superiority for DOA estimation as compared to a scalar sensor array [4, 5]. Since EVSA is sensitive to polarization information, additional polarization phase will be generated when EVSA is adopted for DOA estimation. Thus, the traditional DOA estimation methods such as multiple signal classification (MUSIC) [6] and estimation of signal parameters via rotation invariance techniques (ESPRIT) [7] cannot be directly used for the DOA estimation with EVSA.

In recent years, the DOA estimation issue with EVSA has been widely studied [8–12]. Wong and Zoltowski [8] proposed a closed-form ESPRIT based method for DOA and polarization estimation with arbitrarily spaced EVSA. Based on Root-MUSIC, a polynomial-rooting method [9] was presented for azimuth-elevation DOA and polarization estimation using dipoles, loops, and/or circularly polarized antennas. A novel self-initiating MUSIC-based direction-finding and polarization-estimation method in spatio-polarizational beamspace was developed in [10] using EVSA. Zheng [11] proposed a high-accuracy DOA estimator by exploiting the coarse-fine estimate combination. In [12], an ESPRIT-based method was proposed for joint DOA-range-polarization estimation for MIMO radar. However, these joint DOA and polarization estimation methods cannot be used for the practical PRDRF system. This is because the methods mentioned above adopt orthogonally oriented multi-component EVSAs and occupy a large space, but the antenna size and layout are generally restricted in the practical PRDRF system. As a result, a flexible antenna arrangement form and an appropriate size of antenna dish are required in the practical PRDRF system [13]. The spatially separated single-component circular electromagnetic vector sensor array (SSSC-EVSA) contains multiple separated dipoles mounted on curved surfaces, which is

---

Received 12 September 2018, Accepted 15 October 2018, Scheduled 25 October 2018

\* Corresponding author: Pinjiao Zhao (zhaopinjiao@hrbeu.edu.cn).

<sup>1</sup> Department of Electronic and Information Engineering, Jinling Institute of Technology, Nanjing 211169, China. <sup>2</sup> No. 8511 Research of Institute of CASIC, Nanjing 210007, China.

flexible and space-saving. To the best of our knowledge, there is nearly no research on joint DOA and polarization estimation using SSSC-EVSA. The long vector-based MUSIC (LV-MUSIC) [14, 15] is one of the most typical DOA and polarization parameter estimation methods, which can be directly applied to the SSSC-EVSA. Unfortunately, the LV-MUSIC method involves computationally intensive four-dimensional (4D) spectral search.

This paper develops a dimensionality reduction MUSIC (DR-MUSIC) method for joint DOA and polarization estimation based on SSSC-EVSA, in which 4D spectral search is avoided, and the computational complexity is reduced accordingly. The DOAs of impinging sources are resolved by 2D spectral search, and polarization parameters are estimated via the generalized eigenvector of matrix pencil. By exploiting the differences between polarization parameters of radar and decoy, the estimated polarization parameters are used for recognition of target radar and decoy. Moreover, we specially consider the phase inconsistency among multi-channels by simulation, which usually exists in the practical PRDRF system.

## 2. ARRAY AND SIGNAL MODEL

For illustration purposes an 8-element SSSC-EVSA sketch and its corresponding cross-sectional diagram are taken as an example which are respectively shown in Figure 1(a) and Figure 1(b). For an  $M$ -element SSSC-EVSA, we define the positive direction of every antenna being the right side of the opened bulge. Then, the antenna pointing angle  $\beta_m$  refers to the angle between positive  $x$ -axis and positive direction of the  $m$ th antenna.

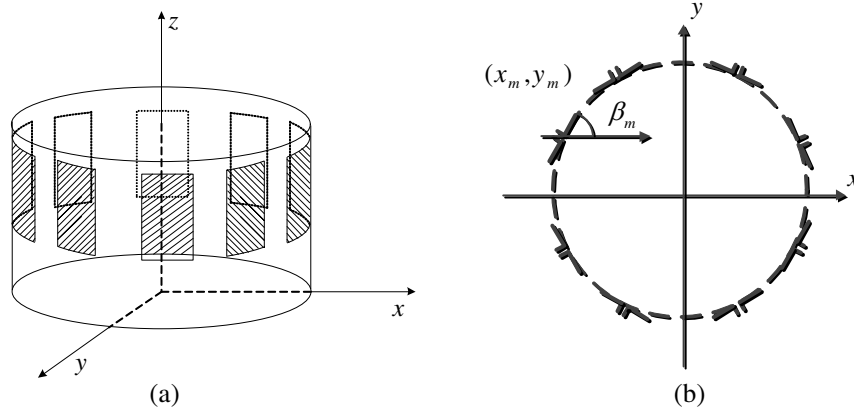


**Figure 1.** SSSC-EVSA model. (a) The sketch map, (b) cross-sectional diagram.

Consider  $K$  completely polarized far-field narrowband transverse electromagnetic (TEM) waves from directions  $(\theta_k, \varphi_k)$  for  $k = 1, 2, \dots, K$  with the carrier wavelength  $\lambda$  impinging on the SSSC-EVSA. The array output vector  $\mathbf{x}(t)$  at time  $t$  is written as

$$\mathbf{x}(t) = \mathbf{A}(\theta, \varphi, \varpi, \varepsilon)\mathbf{s}(t) + \mathbf{n}(t) \quad (1)$$

where  $\mathbf{s}(t)$  is the source vector, and  $\mathbf{n}(t)$  is the additive white noise vector. The array manifold matrix  $\mathbf{A}(\theta, \varphi, \varpi, \varepsilon)$  is an  $M \times K$  array with  $\theta \in [-\pi, \pi]$ ,  $\varphi \in [0, \pi/2]$ ,  $\varpi \in [-\pi/2, \pi/2]$  and  $\varepsilon \in [-\pi/4, \pi/4]$  being the azimuth angle elevation angle, polarization angle and ellipticity angle, respectively.

The  $k$ th column of  $\mathbf{A}(\theta, \varphi, \varpi, \varepsilon)$  can be expressed as

$$\mathbf{A}_k(\theta, \varphi, \varpi, \varepsilon) = \mathbf{a}_k(\theta, \varphi)\mathbf{G}(\beta)\mathbf{B}_k(\theta, \varphi, \varpi, \varepsilon) \quad (2)$$

where  $\mathbf{a}_k(\theta, \varphi)$  denotes an  $M \times 1$  spatial steering vector, and the  $m$ th ( $m = 1, 2, \dots, M$ ) row of  $\mathbf{a}_k(\theta, \varphi)$  is given as

$$a_m(\theta_k, \varphi_k) = \exp[-j2\pi/\lambda(x_m \cos \varphi_k \cos \theta_k + y_m \cos \varphi_k \sin \theta_k)] \quad (3)$$

where  $(x_m, y_m)$  denotes the Cartesian coordinates of the  $m$ th antenna node.

$\mathbf{G}(\beta)$  is called polarization sensitive matrix, which is defined as

$$\mathbf{G}(\beta) = \begin{bmatrix} \cos \beta_1 & \cos \beta_2 & \dots & \cos \beta_M \\ \sin \beta_1 & \sin \beta_2 & \dots & \sin \beta_M \end{bmatrix}^T \quad (4)$$

$\mathbf{B}_k(\theta, \varphi, \varpi, \varepsilon)$  is called polarization steering vector, which comprises both angle and polarization information. For the convenience of analysis,  $\mathbf{B}_k(\theta, \varphi, \varpi, \varepsilon)$  can be transformed into the product of two matrices, in which one contains only angle information, and the other contains only polarization information, i.e.,

$$\mathbf{B}_k(\theta, \varphi, \varpi, \varepsilon) = \mathbf{V}_k(\theta, \varphi) \mathbf{H}_k(\varpi, \varepsilon) \quad (5)$$

where

$$\mathbf{V}_k(\theta, \varphi) = \begin{bmatrix} -\sin \theta_k & \sin \varphi_k \cos \theta_k \\ \cos \theta_k & \sin \varphi_k \sin \theta_k \end{bmatrix} \quad (6)$$

$$\mathbf{H}_k(\varpi, \varepsilon) = \begin{bmatrix} \cos \varpi_k \cos \varepsilon_k - j \sin \varpi_k \sin \varepsilon_k \\ \sin \varpi_k \cos \varepsilon_k + j \cos \varpi_k \sin \varepsilon_k \end{bmatrix} \quad (7)$$

Without loss of generality, we assume that  $\mathbf{s}(t)$  and  $\mathbf{n}(t)$  are the zero-mean stationary Gaussian random processes, and the entries of  $\mathbf{s}(t)$  and  $\mathbf{n}(t)$  are uncorrelated with each other. In general, joint DOA and polarization parameter  $\{\theta_k, \varphi_k, \varpi_k, \varepsilon_k, k = 1, 2, \dots, K\}$  estimation based on LV-MUSIC requires computationally expensive 4D spectral search. The objective of the proposed method is to determine the DOA and polarization parameters through dimensionality reduction.

### 3. DOA AND POLARIZATION ESTIMATION BASED ON DR-MUSIC

The covariance matrix of  $\mathbf{x}(t)$  is calculated as

$$\mathbf{R} = E [\mathbf{x}(t) \mathbf{x}^H(t)] = \mathbf{A}(\theta, \varphi, \varpi, \varepsilon) \mathbf{R}_s \mathbf{A}^H(\theta, \varphi, \varpi, \varepsilon) + \sigma_n^2 \mathbf{I} \quad (8)$$

By performing eigenvalue decomposition (EVD) on  $\mathbf{R}$ , we have

$$\mathbf{R} = \mathbf{E}_s \mathbf{\Lambda}_s \mathbf{E}_s^H + \mathbf{E}_n \mathbf{\Lambda}_n \mathbf{E}_n^H \quad (9)$$

where  $\mathbf{\Lambda}_s$  and  $\mathbf{\Lambda}_n$  are two diagonal matrices that are constructed by the  $K$  largest eigenvalues and the remaining  $M - K$  eigenvalues, respectively.  $\mathbf{E}_s$  and  $\mathbf{E}_n$  are respectively called source subspace and noise subspace constructed by the eigenvectors corresponding to  $\mathbf{\Lambda}_s$  and  $\mathbf{\Lambda}_n$ .

Based on the LV-MUSIC method, cost function is constructed as

$$\mathbf{Q}(\theta, \varphi, \varpi, \varepsilon) = \|\mathbf{E}_n \mathbf{A}(\theta, \varphi, \varpi, \varepsilon)\|_2^2 = \mathbf{A}^H(\theta, \varphi, \varpi, \varepsilon) \mathbf{E}_n \mathbf{E}_n^H \mathbf{A}(\theta, \varphi, \varpi, \varepsilon) \quad (10)$$

It can be seen from Eq. (10) that the joint DOA and polarization estimation based on the LV-MUSIC method involves 4D spectral search, and the computational complexity is tremendous. In order to reduce the computational complexity, the following transformation has been performed on  $\mathbf{Q}(\theta, \varphi, \varpi, \varepsilon)$ , where 4-D MUSIC spectral search can be transformed into 2-D search. Specifically, we denote  $\mathbf{D}_k(\theta, \varphi) = \mathbf{a}_k(\theta, \varphi) \mathbf{G}(\beta) \mathbf{V}_k(\theta, \varphi)$ , and Eq. (2) can be rewritten as

$$\mathbf{A}_k(\theta, \varphi, \varpi, \varepsilon) = \mathbf{D}_k(\theta, \varphi) \mathbf{H}_k(\varpi, \varepsilon) \quad (11)$$

Combining Eq. (10) and Eq. (11), we have

$$\mathbf{Q}(\theta, \varphi, \varpi, \varepsilon) = \mathbf{A}^H(\theta, \varphi, \varpi, \varepsilon) \mathbf{E}_n \mathbf{E}_n^H \mathbf{A}(\theta, \varphi, \varpi, \varepsilon) = \mathbf{H}^H(\varpi, \varepsilon) \mathbf{W}(\theta, \varphi) \mathbf{H}(\varpi, \varepsilon) \quad (12)$$

where  $\mathbf{W}(\theta, \varphi) = \mathbf{D}^H(\theta, \varphi) \mathbf{E}_n \mathbf{E}_n^H \mathbf{D}(\theta, \varphi)$  is referred as the signal component of cost function. Since  $\mathbf{H}(\varpi, \varepsilon)$  is a full-rank matrix, rank deficiency would occur to  $\mathbf{W}(\theta, \varphi)$  when the values of  $\theta, \varphi$  are from actual direction of the incident sources. Then, the DOA estimation  $\{\theta_k, \varphi_k\}_{k=1}^K$  can be obtained by

$$f^{-1}(\theta, \varphi) = \|\mathbf{W}(\theta, \varphi)\| \quad (13)$$

It is noted that the DR-MUSIC method only requires 2D spectral search, which is computationally efficient as compared with the LV-MUSIC method. In the practical PRDRF system, DR-MUSIC can

be performed by parallel processing for further reducing running time, where searching zone can be divided into several small intersecting zones.

For the polarization parameter estimation, we construct matrix pencil as follows:

$$\aleph(\theta, \varphi) = \{\mathbf{W}(\theta, \varphi), \mathbf{D}^H(\theta, \varphi)\mathbf{D}(\theta, \varphi)\} \quad (14)$$

For the actual direction of the incident sources, the minimum generalized eigenvalue of  $\aleph(\theta, \varphi)$  approximates zero. Then, the corresponding generalized eigenvector  $\mathbf{v}_k$  is proportional to  $\mathbf{H}(\varpi_k, \varepsilon_k)$ , i.e.,  $\mathbf{v}_k \propto \mathbf{H}_k(\varpi, \varepsilon)$ .

According to Eq. (7),  $\mathbf{H}_k(\varpi, \varepsilon)$  can be rewritten as

$$\mathbf{H}_k(\varpi, \varepsilon) = \begin{bmatrix} \cos \varpi_k & -\sin \varpi_k \\ \sin \varpi_k & \cos \varpi_k \end{bmatrix} \begin{bmatrix} \cos \varepsilon_k \\ j \sin \varepsilon_k \end{bmatrix} = \begin{bmatrix} \cos \gamma_k \\ \sin \gamma_k e^{j\eta_k} \end{bmatrix} \quad (15)$$

where  $\gamma_k$  and  $\eta_k$  ( $k = 1, 2, \dots, K$ ) denote the auxiliary polarization angle and polarization phase difference, respectively.

The estimates of  $\gamma_k$  and  $\eta_k$  are respectively given as

$$\hat{\gamma}_k = \arctan(|\mathbf{v}_k(2)|/|\mathbf{v}_k(1)|) \quad (16)$$

$$\hat{\eta}_k = \angle(\mathbf{v}_k(2)/\mathbf{v}_k(1)) \quad (17)$$

Finally, in view of the relationship among  $\varpi_k, \varepsilon_k, \gamma_k$  and  $\eta_k, \hat{\varpi}_k, \hat{\varepsilon}_k$  can be obtained via

$$\tan 2\hat{\varpi}_k = \tan 2\hat{\gamma}_k \cos \hat{\eta}_k \quad (18)$$

$$\sin 2\hat{\varepsilon}_k = \sin 2\hat{\gamma}_k \sin \hat{\eta}_k \quad (19)$$

**Remark 1:** In modern electronic warfare, radar and decoys generally exist simultaneously, which makes it difficult to distinguish them only according to the DOA estimates. The effective polarization parameter estimates provide a new approach for distinguishing radar and decoys. In general, the polarization parameters of the decoys are constants, while the polarization parameters of the target radar vary with time randomly. Thus, the polarization estimation can be utilized for resisting decoy jamming.

**Remark 2:** In the practical passive radar direction finding system, the phase inconsistency [16] among multi-channels always exists. Using channel error correction method can reduce the inconsistency, but it cannot be completely avoided. Considering the phase inconsistency among multi-channels, Eq. (1) can be revised as  $\mathbf{x}(t) = \mathbf{C}_{\Delta\Phi}\mathbf{A}(\theta, \varphi, \varpi, \varepsilon)\mathbf{s}(t) + \mathbf{n}(t)$ , where  $\mathbf{C}_{\Delta\Phi} = \text{diag}(C_{\Delta\Phi_1}, C_{\Delta\Phi_2}, \dots, C_{\Delta\Phi_M})$  is the  $M \times M$  phase inconsistency matrix and  $C_{\Delta\Phi_m} = \exp(-j\Phi_m)$  with  $\Phi_m$  ( $m = 1, 2, \dots, M$ ) being the phase difference between the  $m$ th antenna and the reference antenna. The estimation performance under this circumstance will be studied via simulations, see Section 4.2 for detail.

**Remark 3:** In practical engineering applications, real-time is an important evaluation criterion to measure the performance of the system. In the method level, the complexity affects the real-time performance of the system seriously. Here we compare the computational complexity of the DR-MUSIC and LV-MUSIC methods. Assuming that the antenna number is  $M$ , the source number is  $K$ , and the snapshot number is  $T$ . For the DR-MUSIC method, the numbers of 2D spectral search points for  $\theta$  and  $\varphi$  are respectively denoted as  $n_\theta$  and  $n_\varphi$ . For the LV-MUSIC method, the numbers of 4D spectral search points for  $\theta, \varphi, \varpi$  and  $\varepsilon$  are respectively denoted as  $n_\theta, n_\varphi, n_\varpi$  and  $n_\varepsilon$ . For the reason that a large portion of the computational burden is occupied by the multiplication operations, addition operations are negligible. The main computational complexity of the DR-MUSIC and LV-MUSIC methods is listed in Table 1. It can be seen that the DR-MUSIC method is much more computationally efficient than the LV-MUSIC method.

## 4. SIMULATION RESULTS

In this section, several simulations are presented to illustrate the DOA and polarization estimation performance of the proposed DR-MUSIC method, in which the LV-MUSIC method is used for comparison.

**Table 1.** Computational complexity of DR-MUSIC and LV-MUSIC methods.

Methods	EVD	Covariance	Spectral Search
DR-MUSIC	$M^3$	$M^2T$	$(1 + \frac{360}{n_\theta})(1 + \frac{90}{n_\varphi})(M^2 + M)$
LV-MUSIC	$M^3$	$M^2T$	$(1 + \frac{360}{n_\theta})(1 + \frac{90}{n_\varphi})(1 + \frac{160}{n_\varpi}) \times (1 + \frac{90}{n_\varepsilon})(M^2 + M)$

**4.1. Ideal Cases (No Phase Inconsistency among Multi-channels)**

**Simulation 1:** Effectiveness of the DR-MUSIC

Assume that two sources parameterized by  $(25^\circ, 80^\circ, 45^\circ, 10^\circ)$  and  $(185^\circ, 70^\circ, 34^\circ, 20^\circ)$  impinging on an 8-element SSSC-EVSA. The spatial spectrum and the corresponding contour map of the DR-MUSIC with the fixed SNR being 10 dB and snapshot number being 300 are respectively shown in Figure 2(a) and Figure 2(b). The results in Figure 2(a) and Figure 2(b) show that the spectrums have two sharp peaks at the location of two impinging sources, which demonstrate the effectiveness of the DR-MUSIC method.

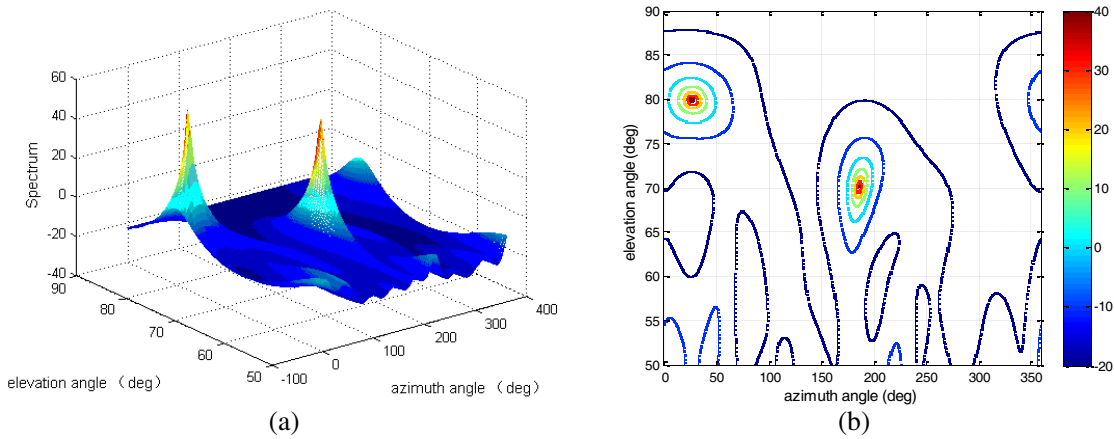


**Figure 2.** Spatial spectrum and contour map of DR-MUSIC. (a) Spatial spectrum of DR-MUSIC, (b) contour map of spatial spectrum.

To demonstrate the computational efficiency of the proposed method, we evaluate the averaged CPU times (in MATLAB 2014 (a) on a 3.2 GHz 4GB PC) of the DR-MUSIC and LV-MUSIC methods over 100 independent Monte Carlo trials, and the results are presented in Table 2. As can be seen from Table 2, the LV-MUSIC method is more time consuming than the DR-MUSIC. This is mainly attributed to that the LV-MUSIC requires computationally intensive 4D spectral search, while the DR-MUSIC only requires 2D spectral search.

**Table 2.** Averaged CPU times.

Methods	Time (sec)
DR-MUSIC	1.4761
LV-MUSIC	4.9267

**Simulation 2:** Estimation performance *versus* the number of array elements and the number of impinging sources

In order to evaluate the estimation performance of the DR-MUSIC method, 100 independent Monte Carlo trials are conducted. The root mean squared error (RMSE) [17] of azimuth angle and elevation angle (or polarization angle and ellipticity angle) for the  $k$ th impinging sources is chosen as an important performance metric, which is defined as

$$RMSE_k = \sqrt{\frac{1}{100} \sum_{n=1}^{100} (\hat{\kappa}_{n,k} - \kappa_{n,k})^2 + (\hat{\tau}_{n,k} - \tau_{n,k})^2} \quad (20)$$

where  $\hat{\kappa}_{n,k}$  is the estimate of  $\kappa_{n,k}$ , and  $\hat{\tau}_{n,k}$  is the estimate of  $\tau_{n,k}$  for the  $n$ th Monte Carlo trial. Specifically, when  $\kappa_{n,k}$  denotes azimuth angle,  $\tau_{n,k}$  denotes elevation angle; when  $\kappa_{n,k}$  denotes polarization angle,  $\tau_{n,k}$  denotes ellipticity angle.

In the second simulation, we investigate the influence of the number of array elements and the number of impinging sources on the estimation performance of the DR-MUSIC method. The SNR and snapshot number are respectively fixed at 10 dB and 300. Figure 3(a) plots the RMSEs of DOA estimates versus the number of array elements ranging from 3 to 8 with two impinging sources from  $(25^\circ, 80^\circ, 45^\circ, 10^\circ)$  and  $(185^\circ, 70^\circ, 34^\circ, 20^\circ)$ . Figure 3(b) plots the RMSEs of DOA estimates versus the number of impinging sources with the 8-element SSSC-EVSA, where the RMSE is the average of multiple  $RMSE_k$  (see Eq. (20)) corresponding to the  $k$ th impinging source. It can be seen from Figure 3(a) that the DOA estimation accuracy tends to improve with the increase of the number of array elements, and the DOA estimation performance degrades seriously when the number of array elements is 3. Figure 3(b) shows that the DOA estimation accuracy tends to decrease with the increase of the number of impinging sources, and the RMSE increases obviously when the number of impinging sources reaches 5.

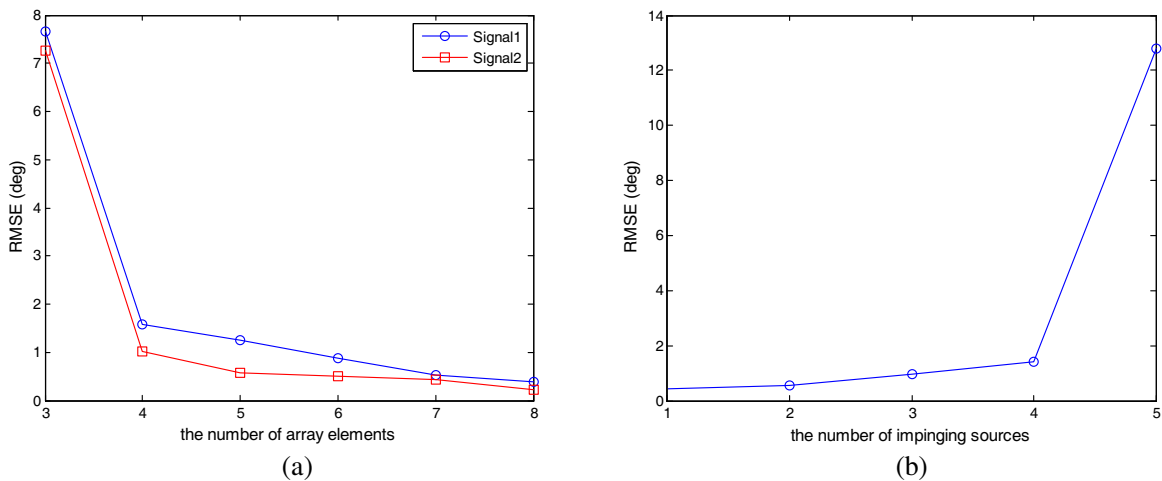


**Figure 3.** DOA estimation performance of DR-MUSIC. (a) RMSEs of DOA estimates versus the number of array elements, (b) RMSEs of DOA estimates versus the number of impinging sources.

### Simulation 3: Performance comparison of the DR-MUSIC and LV-MUSIC

In simulation 3, the simulation settings are the same as those of simulation 1, except the SNR and snapshot number. Figure 4(a) and Figure 4(b) plot RMSEs of DOA and polarization parameter estimates *versus* SNR with fixed snapshot number 300, respectively. Figure 4(c) and Figure 4(d) plot RMSEs of DOA and polarization parameter estimates *versus* snapshot number with fixed SNR 10 dB, respectively. As can be seen from Figure 4(a) to Figure 4(d), the estimation accuracy of DOA and polarization parameter tends to improve with the increase of SNR or snapshots, and the DR-MUSIC and LV-MUSIC methods have similar estimation accuracies.

## 4.2. Considering the Phase Inconsistency among Multi-channels

### Simulation 4: Effectiveness of the DR-MUSIC

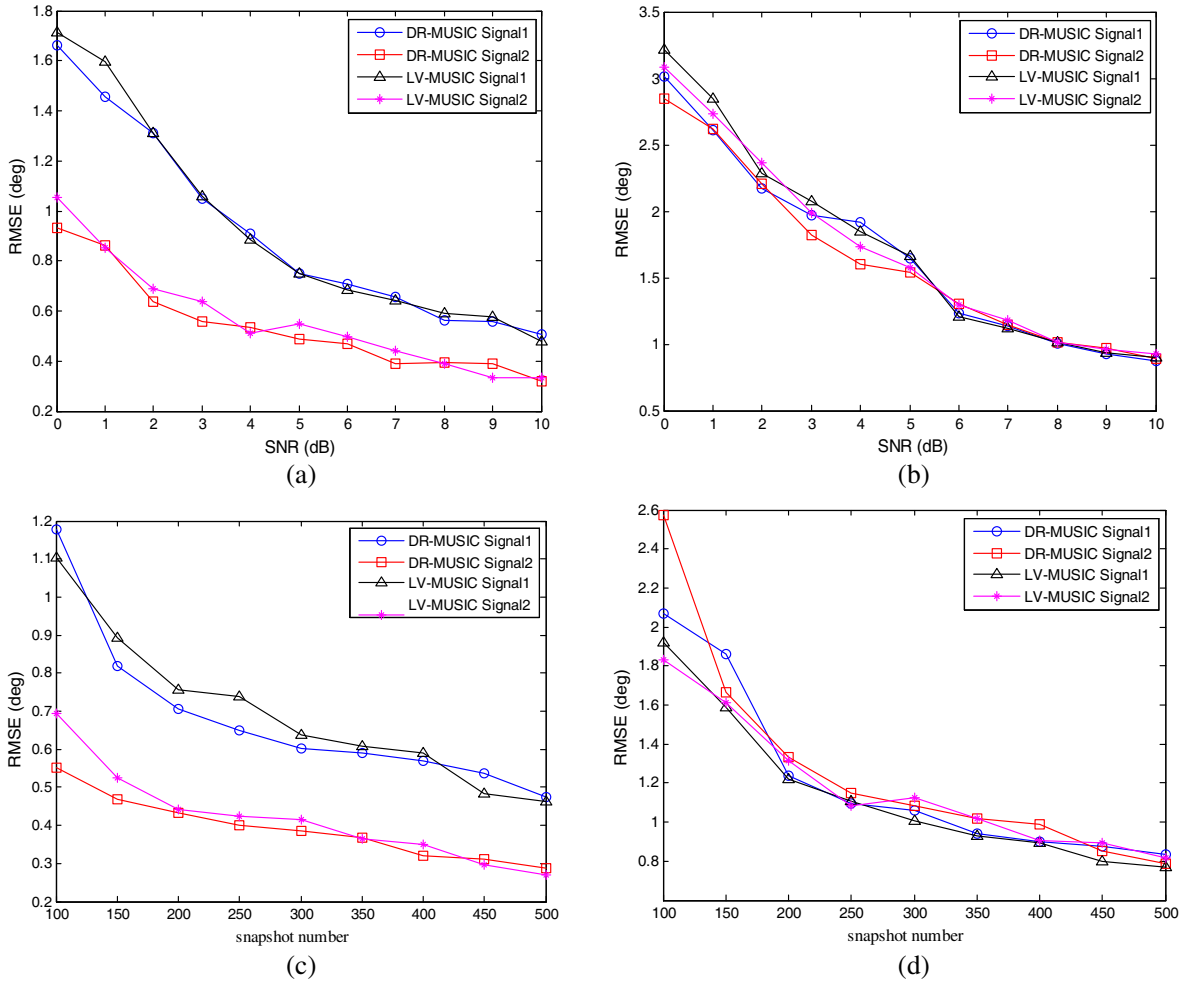


**Figure 4.** RMSEs of DOA and polarization parameter estimates. (a) RMSEs of DOA estimates *versus* SNR with the fixed snapshot number 300, (b) RMSEs of polarization parameter estimates *versus* SNR with the fixed snapshot number 300, (c) RMSEs of DOA estimates *versus* snapshot number with the fixed SNR 10 dB, (d) RMSEs of polarization parameter estimates *versus* snapshot number the fixed SNR 10 dB.

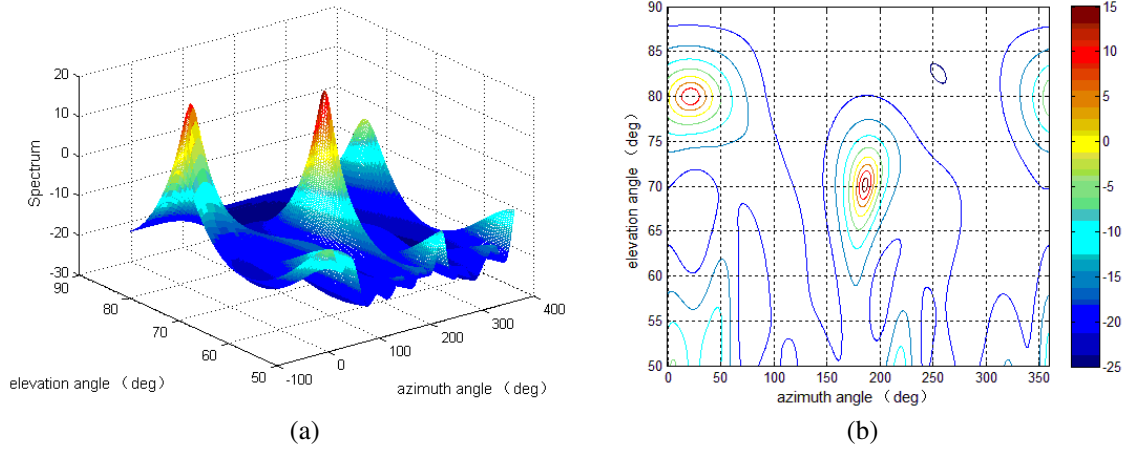
This simulation specially considers the scenario of phase inconsistency among multi-channels by introducing a random phase inconsistency matrix  $C_{\Delta\Phi}$  with the maximum phase difference being  $10^\circ$  ( $\Delta\Phi_{\max} = 10^\circ$ ). The simulation settings are the same as those of simulation 1. The spatial spectrum and the corresponding contour map of DR-MUSIC are respectively drawn in Figure 5(a) and Figure 5(b).

Figure 5(a) and Figure 5(b) show that the DR-MUSIC method can estimate the DOA of target sources correctly when considering phase inconsistency among multi-channels. Compared with Figure 2 and Figure 5, we can see that the peaks in Figure 2 are sharper than those in Figure 5, which implies that the existence of phase inconsistency among multi-channels degrades the DOA estimation performance.

**Simulation 5:** Performance comparison of the DR-MUSIC and LV-MUSIC

Simulation 5 studies the estimation performance of DOA and polarization parameters when considering the phase inconsistency among multi-channels. The RMSE curves of DOA and polarization parameter estimates *versus* SNR are plotted in Figure 6(a) and Figure 6(b), while the RMSE curves of DOA and polarization parameter estimates *versus* snapshot number are plotted in Figure 6(c) and Figure 6(d).

The results from Figure 6(a) to Figure 6(d) illustrate that the DR-MUSIC method can effectively estimate DOA and polarization parameters at existence of random phase inconsistency among multi-



**Figure 5.** Spatial spectrum of the DR-MUSIC considering phase inconsistency among multi-channels. (a) Spatial spectrum of DR-MUSIC, (b) contour map of spatial spectrum.

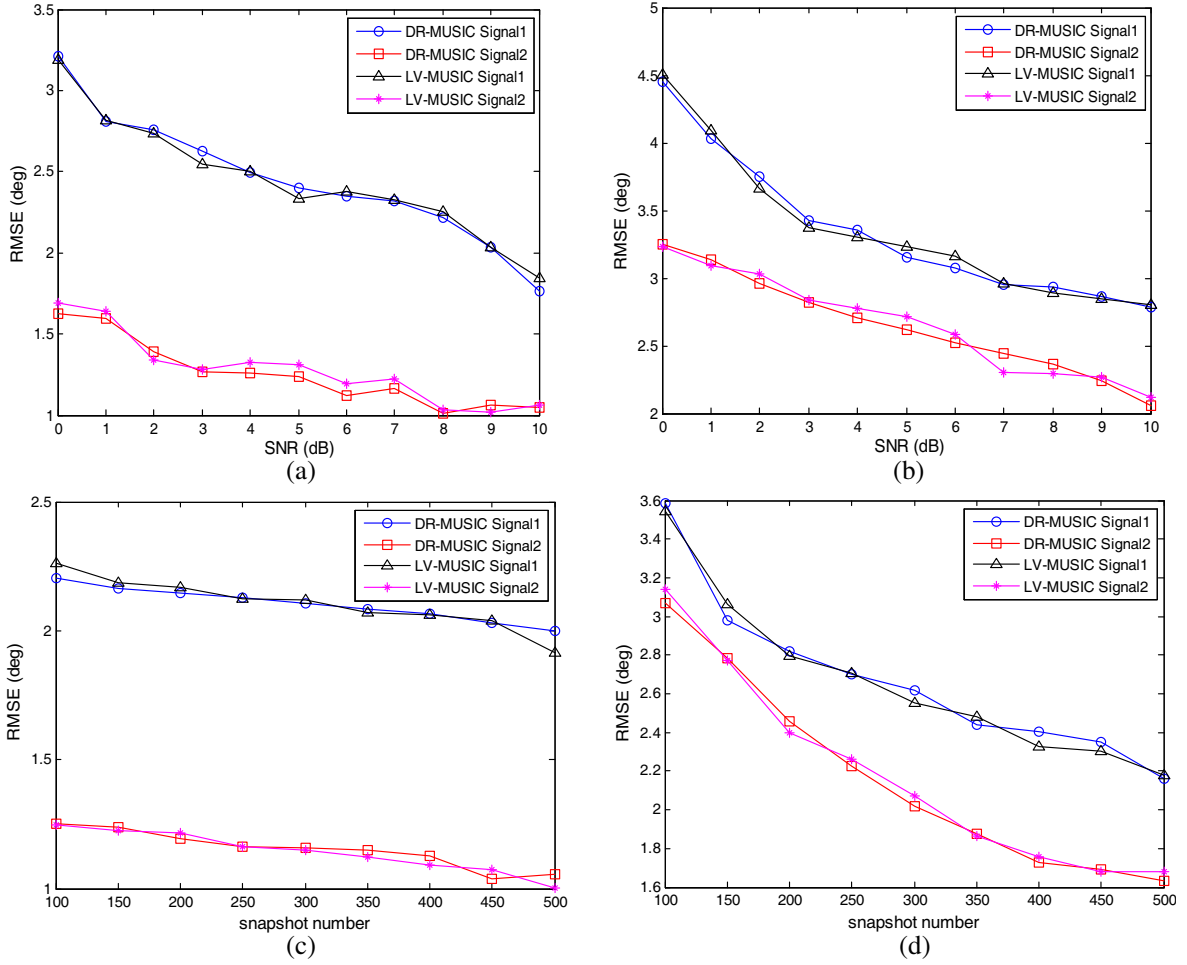


**Figure 6.** RMSEs of DOA and polarization parameter estimates. (a) RMSEs of DOA estimates *versus* SNR with the fixed snapshot number 300, (b) RMSEs of DOA *versus* polarization parameter estimates with the fixed snapshot number 300, (c) RMSEs of DOA estimates *versus* snapshot number with the fixed SNR 10 dB, (d) RMSEs of polarization parameter estimates *versus* snapshot number with the fixed SNR 10 dB.

channels ( $\Delta\Phi_{\max} = 10^\circ$ ). Moreover, compared with Figure 4 and Figure 6, we observe that the estimation accuracy of DOA and polarization parameters when considering phase inconsistency among multi-channels is much lower than those in the ideal cases, thus several channel error correction methods can be introduced to reduce the inconsistency.

## 5. CONCLUSION

In this paper, a DR-MUSIC method based on SSSC-EVSA is developed for joint DOA and polarization estimation. Based on the rank deficiency theory, the DOA and polarization parameters are estimated separately, which avoids 4D spectral search. By constructing the generalized eigenvector of matrix pencil, the polarization parameters are estimated, which can be used for the recognition of radar and decoy. The effectiveness of the DR-MUSIC method is verified by simulations. Moreover, the DR-MUSIC method is also effective when considering the phase inconsistency among multi-channels.

## ACKNOWLEDGMENT

This work was supported by the High Level Talent Research Starting Project of Jinling Institute of Technology (Grant No. jit-b-201724), the Natural Science Foundation of the Jiangsu Province (Project No. BK20161104) and the Six Talent Peaks Project of the Jiangsu Province (Project No. DZXX-022).

## REFERENCES

1. Krim, H. and M. Viberg, "Two decades of array signal processing research: The parametric approach," *IEEE Signal Processing Magazine*, Vol. 13, No. 4, 67–94, 1996.
2. Wu, X., W. P. Zhu, and J. Yan, "A high-resolution DOA estimation method with a family of nonconvex penalties," *IEEE Transactions on Vehicular Technology*, Vol. 67, No. 6, 4925–4938, 2018.
3. Dong, W., M. Diao, and L. Gao, "The direction-of-arrival and polarization estimation using coprime array: A reconstructed covariance matrix approach," *Progress In Electromagnetics Research C*, Vol. 84, 23–33, 2018.
4. Zhao, P., W. Si, G. Hu, et al., "DOA estimation for a mixture of uncorrelated and coherent sources based on hierarchical sparse bayesian inference with a Gauss-Exp-Chi 2 prior," *International Journal of Antennas and Propagation*, Vol. 2018, No. 6, 1–12, 2018.
5. Si, W., P. Zhao, and Z. Qu, "Two-dimensional DOA and polarization estimation for a mixture of uncorrelated and coherent sources with sparsely-distributed vector sensor array," *Sensors*, Vol. 16, No. 6, 789, 2016.
6. Schmidt, R., "Multiple emitter location and signal parameter estimation," *IEEE Transactions on Antennas and Propagation*, Vol. 34, No. 3, 276–280, 1986.
7. Roy, R. and T. Kailath, "ESPRIT-estimation of signal parameters via rotational invariance techniques," *IEEE Transactions on Acoustics, Speech, and Signal Processing*, Vol. 37, No. 7, 984–995, 1989.
8. Wong, K. T. and M. D. Zoltowski, "Closed-form direction finding and polarization estimation with arbitrarily spaced electromagnetic vector-sensors at unknown locations," *IEEE Transactions on Antennas & Propagation*, Vol. 48, No. 5, 671–681, 2000.
9. Wong, K. T., L. Li, and M. D. Zoltowski, "Root-MUSIC-based direction-finding and polarization estimation using diversely polarized possibly collocated antennas," *IEEE Antennas & Wireless Propagation Letters*, Vol. 3, No. 1, 129–132, 2004.
10. Wong, K. T. and M. D. Zoltowski, "Self-initiating MUSIC-based direction finding and polarization estimation in spatio-polarizational beamspace," *IEEE Transactions on Antennas & Propagation*, Vol. 48, No. 8, 1235–1245, 2000.
11. Zheng, G., "A novel spatially spread electromagnetic vector sensor for high-accuracy 2-D DOA estimation," *Multidimensional Systems and Signal Processing*, Vol. 28, No. 1, 23–48, 2017.

12. Li, B., W. Bai, and G. Zheng, "Successive ESPRIT algorithm for joint DOA-range-polarization estimation with polarization sensitive FDA-MIMO radar," *IEEE Access*, Vol. 6, 36376–36382, 2018.
13. Villano, M., F. Colone, and P. Lombardo, "Antenna array for passive radar: Configuration design and adaptive approaches to disturbance cancellation," *International Journal of Antennas and Propagation*, Vol. 2013, No. 3, 1380–1383, Oct. 27, 2013.
14. Guo, W., M. Yang, B. Chen, et al., "Joint DOA and polarization estimation using MUSIC method in polarimetric MIMO radar," *IET International Conference on Radar Systems*, 1–4, 2012.
15. Miron, S., N. Le Bihan, and J. I. Mars, "Vector-sensor MUSIC for polarized seismic sources localization," *EURASIP Journal on Applied Signal Processing*, 74–84, 2005.
16. Liu, S., L. Yang, and S. Yang, "Robust joint calibration of mutual coupling and channel gain/phase inconsistency for uniform circular array," *IEEE Antennas & Wireless Propagation Letters*, Vol. 15, 1191–1195, 2016.
17. Yuan, X., "Estimating the DOA and the polarization of a polynomial-phase signal using a single polarized vector-sensor," *IEEE Transactions on Signal Processing*, Vol. 60, No. 3, 1270–1282, 2012.